Upper critical field divergence induced by mesoscopic phase separation in the organic superconductor $(TMTSF)_2ReO_4$

2008 J. Phys.: Condens. Matter 20 434230

(http://iopscience.iop.org/0953-8984/20/43/434230)

J. Phys.: Condens. Matter **20** (2008) 434230 (5pp) doi:10.1088/0953-8984/20/43/434230

Upper critical field divergence induced by mesoscopic phase separation in the organic superconductor $(TMTSF)_2ReO_4$

C V Colin[1,3], B Salameh[1,4], C R Pasquier[1] and K Bechgaard[2]

[1] Laboratoire de Physique des Solides, Université Paris-Sud, CNRS, UMR 8502, F-91405 Orsay, France
[2] Department of Chemistry, H C Oersted Institute, Universitetsparken 5, DK-2100 Copenhagen, Denmark

Received 7 July 2008
Published 9 October 2008
Online at stacks.iop.org/JPhysCM/20/434230

Abstract
Due to the competition of two anion orders, $(TMTSF)_2ReO_4$ presents a phase coexistence between semiconducting and metallic (superconducting) regions (filaments or droplets) in a wide range of pressures. In this regime, the superconducting upper critical field for H parallel to both c^* and b' axes presents a linear part at low fields followed by a divergence above a crossover field. This crossover corresponds to the 3D–2D decoupling transition expected in filamentary or granular superconductors. The sharpness of the transition also demonstrates that all filaments are of similar sizes and self-organize in a very ordered way. The distance between the filaments and their cross sections are estimated.

Self-organization of electronic charge in strongly correlated electron systems is now commonly observed in many families of materials but the precise texture and the scale at which phase separation occurs is still the subject of a large controversy. In cuprates, the pioneering work of Tranquada *et al* has revealed the existence of spin/charge stripes in $La_2CuO_{4+\delta}$ [1] and the question of its coexistence or competition with superconductivity in underdoped cuprates was addressed later [2]. In these materials, the stripes are formed by the ordered alternation of metallic and insulating 1D ribbons with a lateral extension of typically few lattice parameters. A clear manifestation of these self-organized one-dimensional structures was given by a variation of the in-plane anisotropy of conduction in $YBa_2Cu_3O_y$ ($y = 6.35$–7.0) [3]. From a theoretical point of view, stripes appear upon doping an antiferromagnetic–Mott insulator as an intermediate situation between the fully insulating state stabilized by the long range Coulomb interaction and the metallic state where the kinetic energy is dominant [4–6]. In manganites, phase coexistence plays a key role in the physical properties [7] as the colossal magnetoresistance exhibited by some members of the family [8, 9] may arise from phase separation of ferromagnetic regions embedded in an insulating matrix. In these compounds, the resistivity data were successfully analyzed, at least qualitatively, using a two-fluid model where insulating and metallic conducting paths are in parallel [10]. The real texture in manganites remains a large controversy but a recent scanning tunneling microscopy experiment [11] has opened a new field of investigation of the texture in these compounds. Phase coexistence is not restricted to large electron density systems, as clear signatures of electronic phase coexistence has been reported in an ultrahigh mobility two-dimensional electron gas (2DEG) at the interface of GaAs/GaAlAs heterojunctions which are particularly adapted to the study of quantum Hall effects. The observation of strong anisotropies of conduction in the longitudinal resistivity has been reported at forbidden half-filling factors of the Landau levels from $\nu = 5/2$ to $11/2$ at ultralow temperatures [12]. Here again, the formation of stripe or bubble charge density waves or liquid crystalline phases has been proposed to explain the experimental data [13, 14].

Large electron density organic charge transfer salts also provide model systems in which the question of phase coexistence has been recently addressed. Clear experimental evidence of the texture is still lacking in these materials but the possibility of charge-ordered stripes in α-$(BEDT-TTF)_2I_3$ [15] or θ-$(BEDT-TTF)_2RbZn(SCN)_4$ [16] has been theoretically proposed [17] following NMR

[3] Present address: Institut Néel, CNRS et Université Joseph Fourier, BP 166, F-38042 Grenoble Cedex 9, France.
[4] Present address: Department of Applied Physics, Tafila Technical University, PO Box 179, Tafila 66110, Jordan.

experiments performed in these compounds. Here again, the formation of stripes is related to electron–electron interactions. On the other hand, phase coexistence may also appear due to inhomogeneities which can be introduced in two ways. On the one hand, a small substitution of ClO_4^- anions by ReO_4^- in $(TMTSF)_2ClO_4$ leads to a fast decrease of the critical temperature [18] and a phase repulsion with the competing spin density wave (SDW) state [19]. On the other hand, large SDW domains may be introduced by a high cooling rate in pristine $(TMTSF)_2ClO_4$ [20, 21] or by adjusting the pressure in $(TMTSF)_2PF_6$ [22, 23]. In $(TMTSF)_2PF_6$, these two instabilities coexist in a wide range of pressures and the existence of a macroscopic phase coexistence has been highlighted [22]. The critical temperature is nearly independent of the SDW domain density while the upper critical field [23] or the critical current [22] are strongly affected. The formation of alternating slabs from the two different ground states has therefore been suggested in $(TMTSF)_2PF_6$ to explain the data. In particular, Brazovskii *et al* [24] suggested that the metallic (superconducting) regions are confined in the domain walls of the SDW domains, which are perpendicular to the most conducting direction leading to this slab geometry. Among the whole $(TMTSF)_2X$ family [25], $(TMTSF)_2ReO_4$ presents specific properties: a first-order phase transition is observed at ambient pressure [26] at $T_{AO,2}(P = 1\ \text{bar}) = 180$ K from a metallic state where the tetrahedral anions are disordered toward a semiconducting state characterized by the so-called wavevector $q_2 = (1/2, 1/2, 1/2)$ [27]. As hydrostatic pressure is increased, the semiconducting state is stabilized at lower temperatures but a new anion ordering transition occurs above 7.5 kbar at $T_{AO,3}(P)$ and is stabilized at higher temperatures upon increasing the pressure. This metallic ordered state is characterized by the so-called $q_3 = (0, 1/2, 1/2)$ wavevector [28]. These x-ray measurements also established the coexistence of the two anion orders below $T_{AO,2}(P)$, typically from 7.5 to 11 kbar. Recently, in this compound, we have reported a self-organization of charge in a wide range of pressures [29] due to the competition between the two anion orders q_2 and q_3 [27]. It has been demonstrated that metallic (superconducting) droplets or filaments associated with q_3 order, elongated along the a axis, are embedded in the semiconducting matrix where q_2 order prevails [29]. As the physics involved here is much different from the $(TMTSF)_2PF_6$ case, the nature and the topology of the domains might be strongly different. From resistivity measurements and the use of a Ising model analogy, we have shown that the metallic domains form filaments elongated along the most conducting direction, in contrast to the case of $(TMTSF)_2PF_6$. Moreover, the existence of a possible structural ordering of the filaments can be checked from the superconducting state when the magnetic field is applied perpendicular to the filaments. Indeed, the influence of a regular arrangement of filaments on the upper critical field has been already estimated a long time ago by Turkevich *et al* [30]. A 3D–2D dimensional crossover occurs at a characteristic temperature T^* which depends only on the distance, $d_\perp$, between the filaments in the plane perpendicular to the magnetic field. Above T^*, the normal core of the vortices penetrates the filaments whereas below T^*, they stack between the filaments. This model is, in fact, an extension of the model applied to determine the upper critical field evolution in lamellar superconductors [31] when the magnetic field is perfectly aligned parallel to the superconducting layers and was shown to adjust the data in Nb/Cu multilayers, for instance [32]. Such a dimensional crossover exists also for superconducting droplets embedded in an insulating matrix and the finite size of the droplets leads to a parabolic evolution of the upper critical field at low temperatures [33].

We report here an estimate of the microstructure of the sample in its phase separation regime. Indeed, in $(TMTSF)_2ReO_4$, we will show that, due to the self-organization of charges and the quality of the samples, the dimensional crossover appears clearly on the upper critical field line which establishes a low dispersion in the distances between the superconducting filaments. Then, from the evolution of the upper critical field at lower temperatures, we will extract an estimate of the cross section of the filaments in the $(b–c)$ plane.

The experiments were performed in the pressure range 10–11.8 kbar where both q_2 and q_3 orders coexist. The metallic parts, associated with the q_3 order, present a superconducting transition ($T_c = 1.52$ K) which is nearly pressure-independent [26]. The results are presented on two different samples: on the first one, the current and the magnetic field are applied along the c^* axis, so that ρ_c is measured. On the second one, we performed ρ_a resistivity measurements with the magnetic field, H, applied nearly along the b' axis. The alignment was made by eye and was performed before the application of the hydrostatic pressure. The dimensions of the samples used are typically $2.5 \times 0.2 \times 0.05\ \text{mm}^3$.

Figure 1 presents typical interlayer resistivity versus temperature curves obtained at 10 kbar when the magnetic field is applied along the c^* axis. We first notice that, above T_c and for nearly all magnetic fields, the resistivity presents a metallic character contrary to the SDW-metal phase separation in $(TMTSF)_2PF_6$. This suggests that metallic regions are large and/or a strong coupling between these regions. Above 2 T, the transition is so broad that it is nearly impossible to extract a critical temperature. Then, above 3 T, the rapid increase of the resistance observed might be associated with the field-induced spin density wave states [34]. At each magnetic field, the critical temperature is defined by the onset temperature in a similar way to the previous determination in $(TMTSF)_2PF_6$ [23]. This criterion is justified since this definition also corresponds to the temperature where nonlinearities in the voltage–current characteristics disappear. The magnetic field–temperature phase diagram deduced from these data is shown in figure 2. The same data can be extracted for various pressures and the phase diagram obtained for $P = 11$ kbar is also shown in this figure. At high temperatures, for all pressures, the upper critical field varies smoothly and quasi-linearly with the magnetic field. However, at low temperatures, a drastic upward curvature in the H_{c2} curve is clearly visible which is translated to lower temperatures as pressure is increased. Finally, at $P = 12$ kbar, H_{c2} is

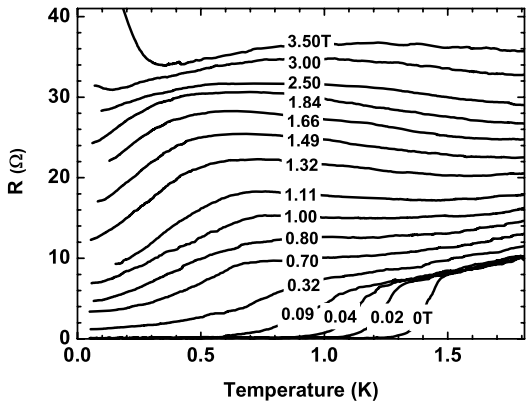

Figure 1. Resistance along the c^* axis versus temperature in $(TMTSF)_2ReO_4$ at $P = 10$ kbar and $H \parallel c^*$. The curves are performed with an applied magnetic field of 0–3.50 T from bottom to top.

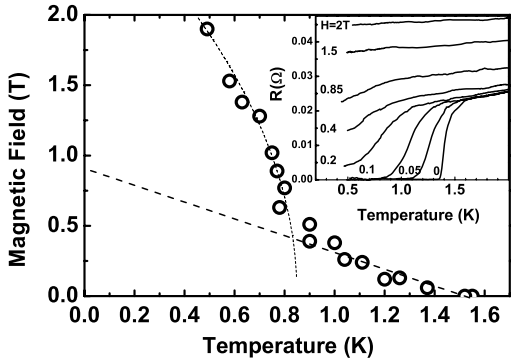

Figure 3. Temperature–magnetic field phase diagram of $(TMTSF)_2ReO_4$ for $P = 10$ kbar and H nearly parallel to b'. The straight line represents the extrapolation of the linear part of the upper critical field while the dotted lines represent the fit of the H_{c2} line with a parabolic law. Inset: resistance versus temperature for H nearly parallel to b'.

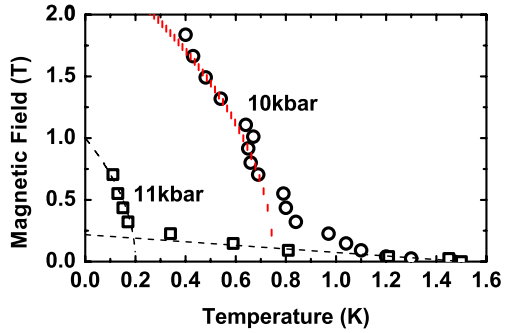

Figure 2. Temperature–magnetic field phase diagram of $(TMTSF)_2ReO_4$ for $P = 10$ kbar (open circles) and 11 kbar (open squares) and $H \parallel c^*$. The straight line represents the upper critical field in the homogeneous state while the dashed lines represent fits of the H_{c2} lines with a parabolic law.

(This figure is in colour only in the electronic version)

quasi-linear with magnetic field: no more divergence from this linear behavior is observed in the explored temperature range. Figure 3 presents the magnetic field–temperature phase diagram for $H \parallel b'$, at $P = 10$ kbar, deduced from the ρ_a resistivity curves obtained at different magnetic fields which are shown in the inset. Here again, just above T_c, the resistivity remains metallic in the whole explored range of magnetic fields. Similarly to $H \parallel c^*$ data, a linear variation of H_{c2} is observed at low fields, which is replaced by a strong upturn of the upper critical field below a characteristic temperature.

These evolutions of the upper critical field with temperature for both field directions are in strong contrast with the reported observations in $(TMTSF)_2PF_6$ where the upturn of the upper critical field is observed starting from the lowest fields [23]. The data may then be analyzed using a different model and it appears clearly that the image of a filamentary superconductor already suggested using resistivity anisotropy data is valid [29]. Since $(TMTSF)_2ReO_4$ is strongly one-dimensional, we will denote by ξ_a, ξ_b and ξ_c the coherence lengths along the a, b' and c^* axes, respectively. In a regular stack of droplets, filaments or slabs, a dimensional crossover in the superconducting state is expected at a fixed temperature T^* defined by

$$\xi_\perp(T^*) = \frac{\xi_\perp(0)}{\sqrt{1 - \frac{T^*}{T_c}}} = \frac{d_\perp}{\sqrt{2}} \qquad (1)$$

where $\xi_\perp(T)$ is the temperature-dependent coherence length perpendicular to the field, H and $d_\perp$ is the distance between the superconducting objects in the plane perpendicular to H. Above this temperature T^*, the superconductor is 3D and the upper critical field varies linearly with temperature like a standard homogeneous superconductor. Below T^*, vortices remain between the filaments and are of Josephson nature [35] and a Lawrence–Doniach model may be applied [36]. In this two-dimensional regime, a divergence of the upper critical field is expected and is limited by finite-size effects, the paramagnetic limit or eventually spin–orbit coupling. The latter possibility is not pertinent in organic conductors made of light elements. However, in strongly one-dimensional systems, a Fulde–Ferrell–Larkin–Ovchinnikov (FFLO) superconducting state [37, 38] may also be considered [39]. However, FFLO superconductivity leads to an inhomogeneous superconducting state in the reciprocal space whereas we are dealing here with phase separation in the real space. Recently, FFLO superconductivity was proposed to explain the experimental data of $(TMTSF)_2ClO_4$ placed in a magnetic field precisely aligned along particular crystallographic directions [40]. A linear variation of the upper critical field was observed in a wide temperature range and a small upturn of the upper critical field was confined to ultralow temperatures, in strong contrast with the data presented here. As a result such an interpretation may be ruled out and a more standard image associated to finite-size effects seems more appropriate. In this case, at high fields when the domains are decoupled (2D regime), a square-root variation of the upper critical field line is expected below T^* including the finite size of the superconducting objects [31, 33]. Assuming spherical metallic grains, Deutscher *et al* estimated the upper critical

field at zero temperature to be given by

$$H_{c2}(0) = \sqrt{\frac{5}{3}}\frac{\Phi_0}{2\pi}\frac{1}{\xi_\perp(0)R}\sqrt{1-2\frac{\xi_\perp^2(0)}{t^2}} \qquad (2)$$

where R is the radius of the grains and t is a characteristic length which measures the Josephson coupling between them. In the ultraweak coupling limit, t is infinite and equation (2) reduces to the standard upper critical field of an individual spherical object [41]. Here, the cross section of the filaments is not a circle but an ellipse. In a first approximation, the previous formula applies if the radius R is replaced by the half-axis of the ellipse perpendicular to the field, $R_\perp$.

In order to determine the precise texture, the coherence lengths have to be determined first. The zero-field linear extrapolation of the upper critical field for $H \parallel c^*$, $H_{c2,c} \approx 0.2$ T is similar to the value obtained for homogeneous superconductivity in $(TMTSF)_2PF_6$ [42] or $(TMTSF)_2ClO_4$ [43] and leads to the determination of $\xi_{\perp,c} = \sqrt{\xi_a\xi_b} \approx 41$ nm deduced from the classical formula: $H_{c2}(0) = \frac{\Phi_0}{2\pi\xi^2}$. However, our zero-field extrapolation of the upper critical field for $H \parallel b'$, which is obtained by extrapolating linearly the upper critical field line from its value at low fields, $H_{c2,b} \approx 0.9$ T, is much smaller than measurements reported in $(TMTSF)_2ClO_4$ or $(TMTSF)_2PF_6$ performed with a perfect alignment of the magnetic field [40, 42–44]. This is due to our experimental set-up which does not allow a perfect alignment of our sample with respect to the b' axis under pressure. We can deduce a rough estimate of the misalignment of our sample to be about 10°, assuming that the upper critical field is identical for $(TMTSF)_2ClO_4$ and $(TMTSF)_2ReO_4$ for $H \parallel b'$. This misalignment is not crucial and in the following we will correct the measurements from this angle. For clarity, we will denote b'' as our direction of measurement. From $H_{c2,b'} = 4$ T [40] which gives an anisotropy ratio $\gamma = H_{c2,b'}/H_{c2,c^*} = 20$, we get $\xi_{\perp,b'} = \sqrt{\xi_a\xi_c} \approx 9$ nm. Using $\xi_a = 100$ nm as in $(TMTSF)_2ClO_4$ [43], we obtain $\xi_b \approx 4.1$ nm and $\xi_c \approx 0.9$ nm which is smaller than the lattice parameter c. In this sense, the estimated value of ξ_c is compatible with the observation of Josephson vortices in $(TMTSF)_2ClO_4$ for H perfectly aligned along the b' axis [45]. The experimental misalignment of the field with respect to the b' axis avoids then to have a mixing of two different physical phenomena. Indeed, the possibility of Josephson vortices between the individual layers, separated by the lattice parameter c, can be ruled out to analyze our data and would have complicated strongly the analysis. The deviation from perfect alignment is sufficiently strong to avoid this 'parasitic' phenomenon here.

We now turn to the determination of the texture at $P = 10$ kbar. For simplicity, in the absence of any x-ray data, we will assume that filaments elongated along the a axis form a rectangular lattice in the b'–c plane following the Deutscher *et al* model [33]. This assumption is justified by both the linear variation at low fields and the square-root variation of the upper critical field and its observations along both directions. As a result, the distance between the filaments and the cross section of each filament is nearly constant over the crystal. We will denote by B and C the distances between the filaments along b' and c^*, respectively. These quantities can be extracted from the H_{c2} lines and using equation (1) with $d_\perp = B$ or C. To define T^*, we use the intersection of the temperature axis with the parabolic fit of the H_{c2} line at low temperatures which gives a more precise determination than any crossover at a finite field. At $P = 10$ kbar, we get $T^* = 0.75$ K and $T^* = 0.85$ K along the c^* and b'' axis, respectively, which leads to $B \approx 80$ nm and $C \approx 50$ nm using only one significant digit.

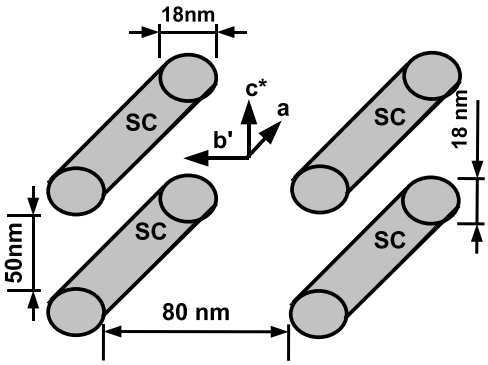

Figure 4. Texture of $(TMTSF)_2ReO_4$ at $P = 10$ kbar deduced from the upper critical field data and assuming a rectangular lattice. SC denotes the superconducting filaments.

Finally, we can estimate the cross section of the filaments at $P = 10$ kbar. In a first step, the coupling between the filaments can be assumed to be very small. From the fits of the low-temperature H_{c2} lines, we can estimate $H_{c2,c}(0) \approx 2.5$ T and $H_{c2,b''}(0) \approx 2.9$ T. Using $\gamma = 20$ and a standard Ginzburg–Landau approximation, we can deduce $H_{c2,b'}(0) \approx 10$ T so that $R_{\perp,c} \approx 9$ nm and $R_{\perp,b'} \approx 9$ nm. One may note that large approximations are made here due to uncertainties in the determinations of both T^* and H_{c2} at low temperatures. The texture proposed at $P = 10$ kbar is depicted in figure 4 assuming a rectangular lattice. The metallic fraction obtained is about 2%, in excellent agreement with the resistivity data [29] considering the crude assumptions made here. We notice that the cross sections of the filaments are of the same order of magnitude as the coherence lengths, justifying the term 'mesoscopic phase separation'. In order to confirm our image, the evolution of the phenomena with increasing pressure has to be clarified. The basic influence of pressure is to increase the amount of the metallic part, which means larger filaments with a smaller distance between them. Smaller B and C parameters manifest by a decreasing temperature T^*. This is effectively observed experimentally. As shown in figure 2, from 10 to 11 kbar, T^* varies from 0.75 to 0.2 K, leading to a decrease of the distance between the filaments from 80 to 60 nm. This shift of T^* is accompanied by a decrease of H_{c2} at zero temperature which implies larger filaments and/or an increased coupling due to a lower distance between the filaments.

In summary, the superconducting data along two field directions has allowed the determination of the texture of a compound, $(TMTSF)_2ReO_4$, in its phase separation regime. The presence of both a linear regime and a parabolic law in the upper critical field curve have demonstrated the regular ordering of the individual filaments. This is a clear signature

of a self-organization of the charge and that the physics studied here is not dominated by defects but only by long range interactions between the domains with a precise orientation of the anions. The data also demonstrate that phase separation occurs at the mesoscopic scale.

Acknowledgments

The authors acknowledge D Jérome for fruitful discussions. We are also grateful to P Auban-Senzier for her assistance with the pressure equipment. This work is supported by the European Community under grant COMEPHS no. NMPT4-CT-2005-517039. CC and BS also acknowledge this grant for financial support.

References

[1] Tranquada J, Sternlieb B, Axe J, Nakamura Y and Uchida S 1995 *Nature* **375** 561
[2] Tranquada J, Axe J, Ichikawa N, Moodenbaugh A, Nakamura Y and Uchida S 1997 *Phys. Rev. Lett.* **78** 338
[3] Ando Y, Segawa K, Komiya S and Lavrov A 2002 *Phys. Rev. Lett.* **88** 137005
[4] Emery V, Kivelson S and Lin H 1990 *Phys. Rev. Lett.* **64** 475
[5] Poilblanc D and Rice T 1989 *Phys. Rev.* B **39** 9749
[6] Zaanen J and Gunnarsson O 1989 *Phys. Rev.* B **40** 9749
[7] Dagotto E, Hotta T and Moreo A 2001 *Phys. Rep.* **344** 1
[8] Tokura Y, Urushibara A, Moritomo Y, Arima T, Asamitsu A, Kido G and Furukawa N 1994 *J. Phys. Soc. Japan* **63** 3931
[9] Tomioka Y and Tokura Y 2002 *Phys. Rev.* B **66** 104416
[10] Mayr M, Moreo A, Vergés J, Arispe J, Feiguin A and Dagotto E 2001 *Phys. Rev. Lett.* **86** 135
[11] Renner C, Aeppli G, Kim B-G, Soh Y-A and Cheong W 2002 *Nature* **416** 518
[12] Lilly M, Cooper K, Eisenstein J and Pfeiffer L 1999 *Phys. Rev. Lett.* **82** 394
[13] Koulakov A, Fogler M and Shklovskii B 1996 *Phys. Rev. Lett.* **76** 499
[14] Moessner R and Chalker J 1996 *Phys. Rev.* B **54** 5006
[15] Takano Y, Hiraki K, Yamamoto H, Nakamura T and Takahashi T 2001 *J. Phys. Chem. Solids* **62** 393
[16] Miyagawa K, Kawamoto A and Kanoda K 2000 *Phys. Rev.* B **62** R7679
[17] Seo H 2000 *J. Phys. Soc. Japan* **69** 805
[18] Joo N, Auban-Senzier P, Pasquier C R, Monod P, Jérome D and Bechgaard K 2004 *Eur. Phys. J.* B **40** 43
[19] Joo N, Auban-Senzier P, Pasquier C R, Jérome D and Bechgaard K 2005 *Eur. Phys. Lett.* **72** 645
[20] Schwenk H, Andres K and Wudl F 1984 *Phys. Rev.* B **29** 500
[21] Pouget J-P, Kagoshima S, Tamegai T, Nogami Y, Kubo K, Nakajima T and Bechgaard K 1990 *J. Phys. Soc. Japan.* **59** 2036
[22] Vuletić T, Auban-Senzier P, Pasquier C, Tomić S, Jérome D, Héritier M and Bechgaard K 2002 *Eur. Phys. J.* B **25** 319
[23] Lee I J, Naughton M J and Chaikin P M 2002 *Phys. Rev. Lett.* **88** 207002
[24] Brazovskii S, Gorkov L and Lebed A 1982 *Sov. Phys.—JETP* **56** 683
[25] Jérome D 2004 *Chem. Rev.* **104** 5565
[26] Parkin S S P, Jérome D and Bechgaard K 1981 *Mol. Cryst. Liq. Cryst.* **79** 213
[27] Moret R, Pouget J-P, Comés R and Bechgaard K 1982 *Phys. Rev. Lett.* **49** 1008
[28] Moret R, Ravy S, Pouget J P, Comés R and Bechgaard K 1986 *Phys. Rev. Lett.* **57** 1915
[29] Colin C, Auban-Senzier P, Pasquier C R and Bechgaard K 2006 *Eur. Phys. Lett.* **75** 301
[30] Turkevich L and Klemm R 1979 *Phys. Rev.* B **19** 2520
[31] Klemm R, Luther A and Beasley M 1975 *Phys. Rev.* B **12** 877
[32] Krasnov V M, Kovalev A E, Oboznov V A and Pedersen N F 1996 *Phys. Rev.* B **54** 15448
[33] Deutscher G, Entin-Wohlman O and Shapira Y 1980 *Phys. Rev.* B **22** 4624
[34] Greene R, Parkin S S P and Schwenk H 1986 *Physica* B **143** 388
[35] Feinberg D and Villard C 1990 *Phys. Rev. Lett.* **65** 919
[36] Lawrence W and Doniach S 1971 *Proc. 12th Int. Conf. on Low Temperature Physics* ed E Kanda, p 361
[37] Fulde P and Ferrell R A 1964 *Phys. Rev.* **135** A550
[38] Larkin A I and Ovchinnikov Y N 1964 *Zh. Eksp. Teor. Fiz.* **47** 113
Larkin A I and Ovchinnikov Y N 1965 *Sov. Phys.—JETP* **20** 762 (Engl. Transl.)
[39] Dupuis N 1995 *Phys. Rev.* B **51** 9074
[40] Joo N *et al* 2006 *Eur. Phys. J.* B **52** 337
[41] de Gennes P and Tinkham M 1964 *Physics (N.Y.)* **1** 107
[42] Lee I J, Naughton M J, Danner G M and Chaikin P M 1997 *Phys. Rev. Lett.* **78** 3555
[43] Murata K, Tokumoto M, Anzai H, Kajimura K and Ishiguro T 1987 *Japan. J. Appl. Phys. Suppl.* **26** 1367
[44] Oh J I and Naughton M J 2004 *Phys. Rev. Lett.* **92** 67001
[45] Mansky P A, Danner G and Chaikin P M 1995 *Phys. Rev.* B **52** 7554